Surface-induced organization of ***n***-alkanes on nanostructured PTFE: II. Brillouin spectroscopic investigations on ***n***-tritriacontane

1997 J. Phys.: Condens. Matter 9 8407

(http://iopscience.iop.org/0953-8984/9/40/008)

J. Phys.: Condens. Matter **9** (1997) 8407–8417. Printed in the UK PII: S0953-8984(97)84248-8

Surface-induced organization of n-alkanes on nanostructured PTFE: II. Brillouin spectroscopic investigations on n-tritriacontane

C Fischer†, J K Krüger† and W Heitz‡

† Fachrichtung Experimentalphysik 10.2, Universität des Saarlandes, Bau 38, Postfach 151150, D-66041-Saarbrücken, Germany

‡ Fachbereich Physikalische Chemie-Polymere, Philipps-Universität Marburg, Germany

Received 13 May 1997

Abstract. The surface-induced orientation of linear molecules on highly oriented, nanostructured polytetrafluoroethylene was used to prepare macroscopic mats of $C_{33}H_{68}$ single crystals. Using high-performance Brillouin spectroscopy, for the first time we were able to determine directly several elastic constants of $C_{33}H_{68}$. The experimental results are discussed in the framework of existing experimental data for the elastic properties of *n*-alkanes.

1. Introduction

Due to their very interesting phase transition behaviour and their model character for the crystalline phases of the corresponding polymer polyethylene, linear *n*-alkanes have been the subject of intense investigation for many years. Even though the structural properties of these systems have meanwhile become well established [1–9], up to now the direct determination of the elastic properties of the crystalline state has been handicapped by the difficulty in obtaining sufficiently defectless single crystals.

The typical habit and plasticity of solution- or melt-grown crystals makes it difficult to prepare suitable crystal cuts to be used in ultrasonic or Brillouin spectroscopic experiments. In spite of this, the lack of suitable samples did not hinder the work carried out to obtain preliminary elastic data for these substances, although it is almost solely indirect experimental methods that have been discussed in the literature [10–15].

The first successful application of a direct method for characterizing the elastic properties of these materials was performed by Krüger *et al* [16, 17] using Brillouin spectroscopy (BS) on a solution-grown $C_{36}H_{74}$ single crystal. Very recently, we proposed a preparation method, based on the surface-induced organization of linear molecules on highly oriented nanostructured polytetrafluoroethylene (the polymer-induced-alignment (PIA) technique), for obtaining oriented crystal plates of *n*-alkanes. This technique, originally introduced by Wittmann and Smith [18], allows one to obtain oriented crystal mats of such very different materials as polymers [19, 20], liquid crystals [21, 22], and *n*-alkanes and perfluoro-alkanes [23–25]).

In the alkane systems investigated up to now ($C_{20}F_{42}$, $C_{24}F_{50}$, $C_{17}H_{36}$, and $C_{25}H_{52}$), the highly oriented PTFE substrate induced a preferential orientation of the crystallites, with the *c*-axis parallel to the direction of preferential orientation of the PTFE molecules, and formed a homogeneous crystal mat suitable for measurement by BS. A comparison with

0953-8984/97/408407+11$19.50

other crystal growth techniques showed that the PIA technique exhibited the same crystal structure as the original material. In fact, the PIA technique forced in $C_{25}H_{52}$ a biaxial orientation of the crystals on the PIA substrate, with the crystallographic *c*-axis as well as the *b*-axis oriented within the film plane [25]. At present, the exact orientation mechanism of linear molecules on PIA substrates is not understood, and is still a subject of intensive investigation [24–27].

For the present study, we chose the *n*-alkane $C_{33}H_{68}$ (*n*-tritriacontane), since the structural properties of $C_{33}H_{68}$ are well established due to the intensive investigations of Strobl and co-workers [3, 4, 12, 13]. In a series of papers, Strobl and co-workers developed a clear molecular picture of the four apparent phases below the melting transition. In contrast to the case for all other *n*-alkane systems characterized up to now, in this material the dynamical so-called 'rotator transition' splits into a series of different phase transitions, where at each transition another kind of molecular dynamics is added. This offers a unique chance to study the influence of the different molecular dynamical processes on the elastic properties of this system. In this paper, we shall restrict our discussion to the room temperature phase of $C_{33}H_{68}$. We shall compare our directly measured elastic data with those indirectly derived from longitudinal acoustic modes (LAM) measurements using Raman scattering [12–15], and we will relate our data to those obtained for $C_{25}H_{52}$ [25]. On the basis of our results, we propose an approach for estimating the elastic constants of odd *n*-alkanes of neighbouring chain lengths.

2. Experimental details

2.1. Sample preparation

2.1.1. Synthesis of n-tritriacontane. $C_{33}H_{68}$ was obtained by reacting 1-bromodocosane (14 g, 0.036 mol), and 1-bromoundecane (42.2 g, 0.18 mol) with sodium (29 g, 1.26 mol) in diethyl ether. The product mixture was precipitated with methanol. C_{12} and C_{22} compounds were removed by distillation. The remaining mixture consists essentially of $C_{33}H_{68}$ and $C_{44}H_{90}$. These two compounds were separated by preparative gel permeation chromatography (GPC), using 2% cross-linked polystyrene as the stationary phase, and chlorobenzene as the solvent at 373 K.

2.1.2. The PIA technique. The PIA technique for preparing sandwich samples has been described in detail in previous papers [21–24]. Here we want only to stress the most important aspects that are of relevance for the present work. The PTFE (PIA) layer, deposited on a conventional glass slide, is molecularly highly oriented, fully crystalline, and has a typical thickness of 20 nm. In order to overcome the non-wetting effect of PTFE with respect to *n*-tritriacontane, we melted the *n*-tritriacontane material between two glass slides, having coated the relevant internal sides with PIA (see also [25]).

In contrast to the observations for $C_{17}H_{36}$ and $C_{25}H_{52}$, the usual fast cooling from the melt yields strongly disordered polydomain films. A closer inspection of the optical properties using a polarization microscope showed that the crystallographic *c*-axes of the domains were randomly distributed in a cone of about 15 degrees around the orientation direction of the PIA molecules. In order to produce a monodomain state, we performed a slow recrystallization from the melt (about 1 K h^{-1}) in a unidirectional temperature gradient with a modified Bridgman crystal growth apparatus [28]. This method drastically reduced the heteronucleation as well as thermomechanical stresses resulting from differences of the thermal expansion coefficients between the sample and the substrate.

As a surprising result, we obtained predominantly macroscopic single-crystalline domains having their crystallographic *c*-axis perpendicular to the PIA substrate. That means that in contrast to previous observations for shorter chain molecules [23–25], the (a, b) plane was the contact plane with the PIA substrate (subsequently these domains are referred to as (a, b) domains). It is worth noting that the crystallographic *a*- and *b*-axes are oriented at random within the PIA substrate plane.

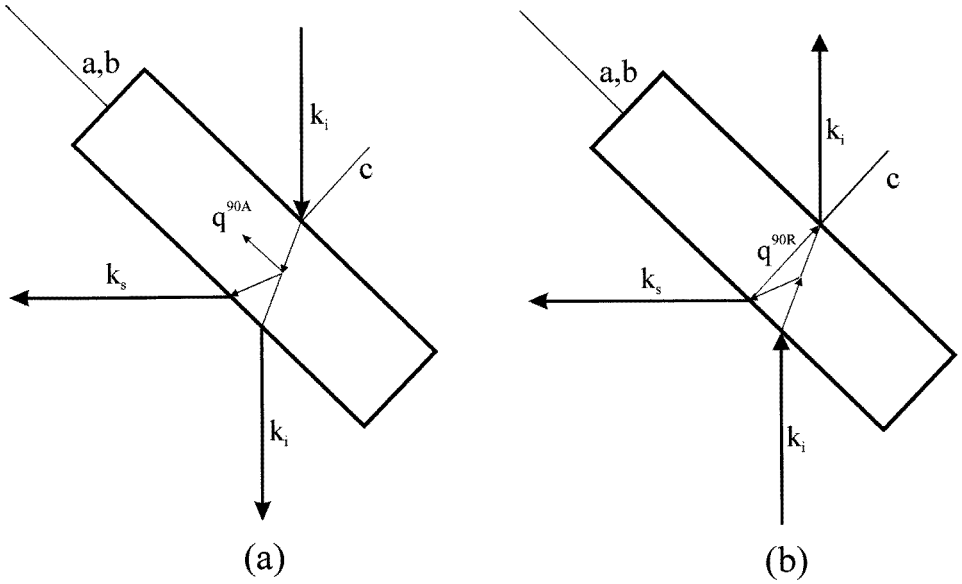

Figure 1. Schematic representations of the 90A (a) and 90R (b) scattering geometries for the film-like $C_{33}H_{68}$ sample. The sample is rotated around the *c*-axis, thus moving $\boldsymbol{q}^{90A}$ within the plane defined by the *a*- and *b*-axes. $\boldsymbol{q}^{90R}$ is always parallel to the *c*-axis. $\boldsymbol{k}_i$: the incident light wave vector; $\boldsymbol{k}_s$: the scattered light wave vector. For further information, see the text.

2.2. Brillouin spectroscopy (BS)

The Brillouin spectrometers used were a five-pass Fabry–Perot interferometer (90A scattering) and a six-pass tandem Fabry–Perot interferometer (90R scattering) with an Ar-ion laser as the light source. The exact experimental set-up is given elsewhere [29]. Figure 1 schematically sketches the principles of the 90A and 90R scattering geometries used. Using film-like samples, angle-resolving BS allows the determination of all or almost all of the components of the elastic stiffness tensor [29].

The relations between the sound velocities and the corresponding phonon frequencies, f^{90A} and f^{90R}, are

$$v^{90A} = \frac{f^{90A}\lambda_0}{\sqrt{2}} \qquad v^{90R} = \frac{f_i^{90R}\lambda_0}{\sqrt{4n_i^2 - 2}} \tag{1}$$

where λ_0 is the laser wavelength in vacuum (514.5 nm) and n_i is the relevant refractive index of the sample. As has been discussed elsewhere, in the case of the 90A scattering geometry, the influence of the birefringence on the acoustic wavelength can be omitted

[30]. The stiffness coefficient, c, related to the measured sound velocity, obeys the relation $c = \rho v^2$ where ρ is the mass density of the material.

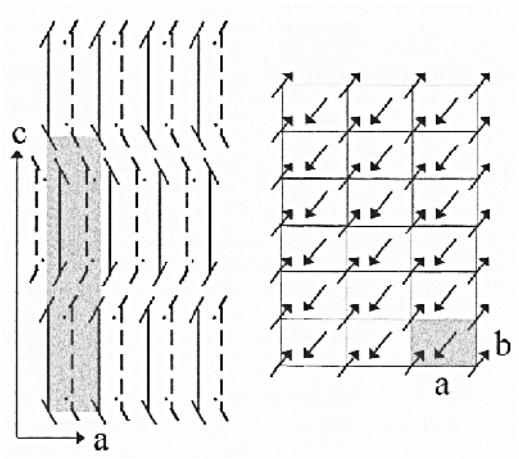

Figure 2. A schematic representation of the room temperature orthorhombic crystal structure of $C_{33}H_{68}$ according to reference [3]. The unit cell is indicated in grey, and the arrows represent the skeletal planes of the all *trans*-molecules; left: viewed along ***b***; right: viewed along ***c***.

After measuring the phonon frequencies for different directions of the phonon wave vector $\boldsymbol{q}^{90A}$ within the (a, b) plane of the sample (the film plane; see also figure 1), the resulting data can be fitted to Christoffel's equation [31], yielding the stiffness coefficients c_{kl} relevant for this crystal cut. The basic relation for the determination of the elastic stiffness tensor $\mathbf{c}$, written in matrix notation, is given by

$$\det(\mathbf{lcl}^{\mathrm{T}} - \mathbf{E}c'(q)) = 0 \tag{2}$$

with

$$\mathbf{l} = \begin{pmatrix} l_1 & 0 & 0 & 0 & l_3 & l_2 \\ 0 & l_2 & 0 & l_3 & 0 & l_1 \\ 0 & 0 & l_3 & l_2 & l_1 & 0 \end{pmatrix}.$$

$\mathbf{c} = \{c_{kl}\}$ is the fourth-rank elastic tensor in shortened 6×6 Voigt notation. $\mathbf{E}$ is the 6×6 unit matrix; l_i $(i = 1, 2, 3)$ are direction cosines which define the direction of the wave vector $\boldsymbol{q} = (l_1, l_2, l_3)$. For the orthorhombic symmetry of $C_{33}H_{68}$ at room temperature, the elastic stiffness coefficients are: $c_{11}, c_{22}, c_{33}, c_{12}, c_{13}, c_{23}, c_{44}, c_{55}, c_{66}$. In our case, the indices 1, 2, 3 refer to the crystallographic axes a, b, c, respectively (see figure 2).

Angle-dependent 90A measurements allowed us to determine the elastic constants c_{11}, c_{22}, c_{12}, and c_{66}. Furthermore, we could determine c_{33} using the 90R scattering geometry. The relative accuracy of the measured sound frequencies is estimated to be better than 0.5%. From the accuracy of the hypersonic frequency data, we deduce the accuracy of the components of the elastic tensor to be about 1.5%.

3. Results and discussion

3.1. The orientational effect of $C_{33}H_{68}$ on PIA substrates

As has already been described in the experimental section, the orientation of *n*-alkanes on nanostructured PTFE strongly depends on the sample preparation conditions and chain

length. While a fast cooling from the melt yields crystals having their molecules more or less oriented along the preferential orientation direction of the PIA molecules, samples slowly crystallized from the melt clearly tend to build up single-crystalline domains in which the molecules are oriented perpendicular to the PIA substrate, i.e. the (a, b) plane is the contact plane. Against the background of these results, we also reinvestigated the crystallization process of $C_{19}H_{40}$ and $C_{25}H_{52}$ on PIA substrates: in fact, we found that extremely slow crystallization from the melt on PIA substrates yields the randomly oriented (a, b) domains for these shorter chain molecules as well. The large (b, c) domains reported for $C_{25}H_{52}$ on PIA [25] can only be obtained if the Bridgman crystallization process starts at a suitably oriented (b, c) nucleus. Unfortunately, the crystallization procedure yielding (b, c) domains in the case of $C_{25}H_{52}$ failed in the case of $C_{33}H_{68}$. We attribute this behaviour to the different and probably more complicated phase sequence of $C_{33}H_{68}$ in comparison to $C_{25}H_{52}$, which has to be passed through in cooling the molten state down to ambient temperature.

These observations clearly demonstrate that, in the case of $C_{33}H_{68}$, there exist concurrent mechanisms for the orientational effect on PIA substrates, which in addition seem to possess different relevant timescales. In the literature, several orientational mechanisms for linear molecules on highly oriented PTFE are discussed, such as epitaxy, grapho-epitaxy, and chemical affinity [18]. Even though we do not know which of the above-mentioned possible mechanisms are responsible for the formation of (b, c) domains in *n*-alkanes, we believe that, for slow cooling rates, the non-wetting properties of PTFE overcompensate these orientation mechanisms, leading to (a, b) domains.

3.2. The elastic properties of $C_{33}H_{68}$

As is usual for the family of odd paraffins, $C_{33}H_{68}$ shows at room temperature an orthorhombic symmetry with the space group $Pcam$. The lattice parameters are [3]: $a = 7.44$ Å, $b = 4.96$ Å, and $c = 87.65$ Å. The corresponding mass density at room temperature is $\rho = 952.8$ kg m^{-3}.

Table 1. Elastic constants of $C_{33}H_{68}$ and $C_{25}H_{52}$.

	$C_{33}H_{68}$ (experiment)	$C_{25}H_{52}$ [25]
ρ (kg m^{-3})	952.8	951.9
c_{11} (GPa)	7.1	7.2
c_{12} (GPa)	4.0	4.1
c_{13} (GPa)	—	2.1
c_{22} (GPa)	7.5	7.4
c_{23} (GPa)	—	2.4
c_{33} (GPa)	44.2	35.0
c_{44} (GPa)	—	2.1
c_{55} (GPa)	—	2.8
c_{66} (GPa)	3.25	2.7

In a first step, an angle-dependent Brillouin measurement was performed. We used the 90A scattering geometry and determined the angle dependence of the sound velocity within the (a, b) plane by turning the sample around its *c*-axis. During the whole measurement, the scattering volume was fixed in the centre of the selected domain. We obtained a representative data set on the quasi-transverse and quasi-longitudinal branches,

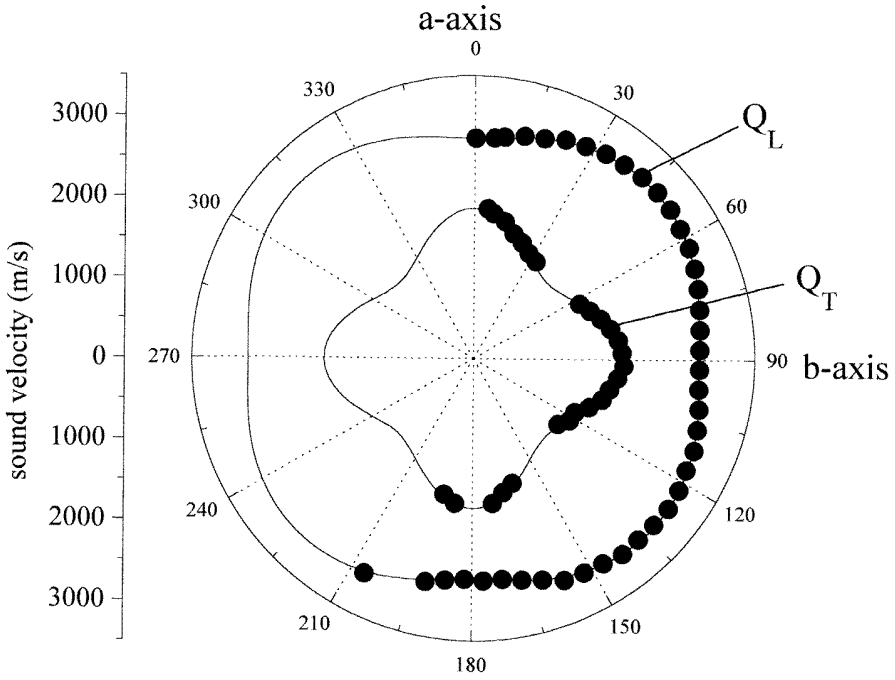

(a)

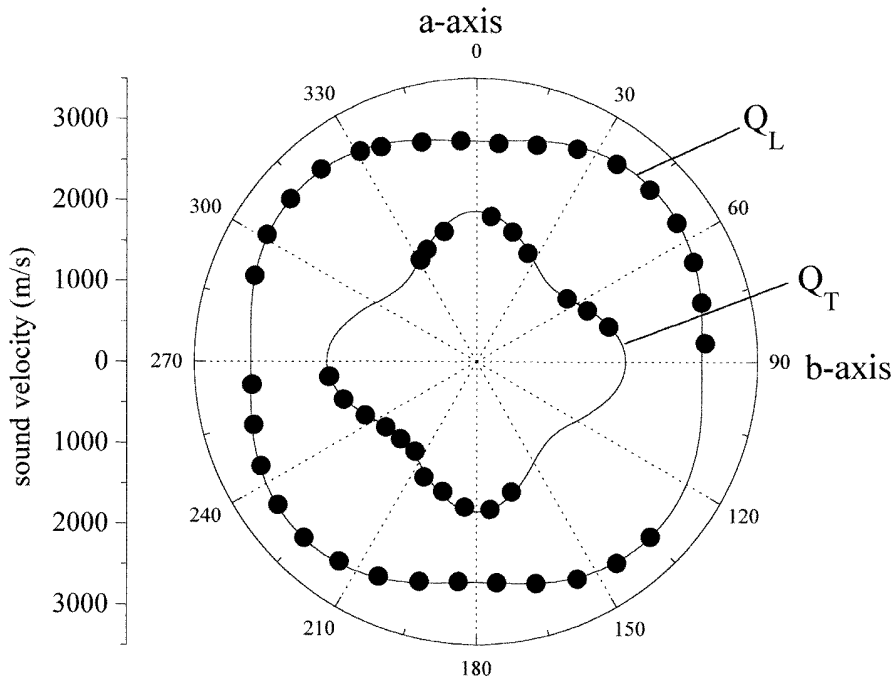

(b)

Figure 3. A sound velocity polar plot of the quasi-transverse (Q_T) and quasi-longitudinal (Q_L) phonon branches within the (a, b) plane of $C_{33}H_{68}$. The full lines refer to a least-squares fit of Christoffel's equation. (a) First sample. (b) Second sample.

which allowed us to directly evaluate the stiffness constants c_{11}, c_{22}, c_{12}, and c_{66}. The corresponding sound velocity polar plot is shown in figure 3(a). The related elastic constants, obtained by a non-linear least-squares fit to the experimental data, are given in table 1. The measurement was repeated with a second sample in order to verify the results obtained for the first sample. As can be seen from figure 3(b), the second measurement completely confirmed the first data set.

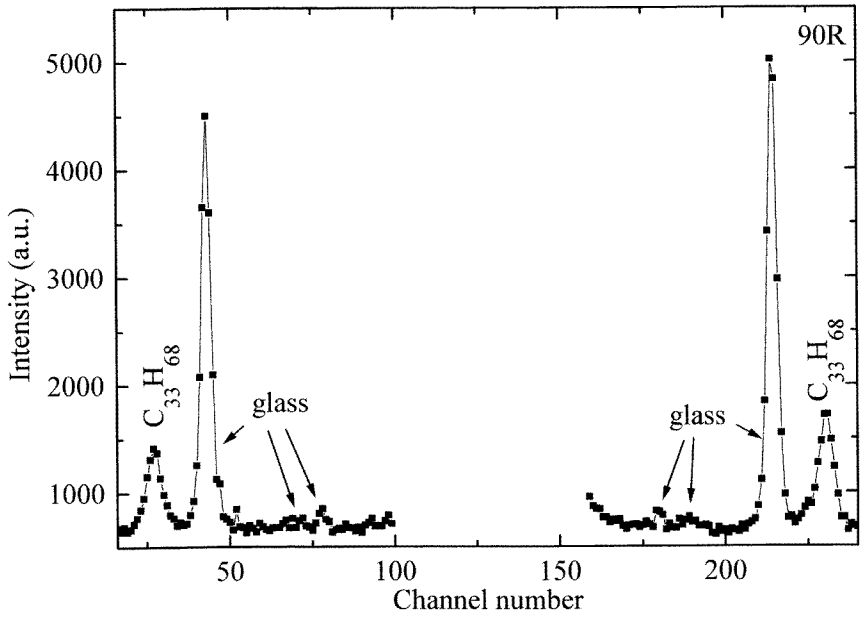

Figure 4. A 90R Brillouin spectrum of $C_{33}H_{68}$ recorded with a six-pass tandem Brillouin spectrometer (scaling factor: 0.351 GHz/channel). As well as the longitudinal Brillouin lines of $C_{33}H_{68}$, Brillouin lines of the glass substrate are also visible. For technical reasons, the central Rayleigh line is not shown.

In order to determine the elastic constant c_{33}, we performed a 90R measurement on the first sample. Making 90R measurements on such thin samples is a difficult task. Because of this, we used the tandem Brillouin spectrometer for this purpose, since it has an enhanced contrast in comparison to our five-pass spectrometer. As already mentioned above, in this scattering geometry, the acoustic wave vector is directed perpendicularly to the film plane, i.e. parallel to the chain direction of the all *trans*-molecules (the crystallographic c-axis). Since the relative orientation of the electric field vector versus the crystallographic a- or b-axis was not known, we used for the determination of the acoustic wavelength the average refractive index $n_i = (n_a + n_b)/2 = 1.521$ [3]. This is thought to be a good estimate for the relevant refractive index, since n_a and n_b differ only slightly. The corresponding 90R Brillouin spectrum is shown in figure 4. As expected, apart from the Brillouin lines of the sample, there also appear the longitudinal and transverse Brillouin lines of the glass substrate.

In table 1 we compare the elastic data for $C_{33}H_{68}$ with those for $C_{25}H_{52}$. At first sight, it is astonishing that the experimental values of c_{11}, c_{22}, and c_{12} are nearly the same, in spite of the fact that the two alkanes differ in chain length by about 25%. We explain this as follows: in the crystallographic (a, b) plane, the elastic properties are mainly determined by the

weak van der Waals interaction forces between neighbouring molecules. The inter-lamellar interaction forces (interactions between methylene end-groups of the stacked lamellae) are also of van der Waals type, and therefore assumed to be of the same order of magnitude as the interaction force within a lamella in the (a, b) plane [25]. Correspondingly, it is not surprising that the longitudinal elastic properties within the (a, b) plane do not strongly depend on the chain length, and this is exactly what is observed. However, the apparent difference between the shear constants c_{66} seems to reflect the influence of the concentration of the inter-lamellar layers within the scattering volume on the elastic shear constant c_{66}.

Brillouin investigations of ultra-drawn polyethylene with fibre symmetry yield $c_{11} = 7.4$ GPa [29]. Even though this value reflects an orientation average over the quasi-longitudinal modes propagating within the (a, b) plane, this value is in perfect agreement with those for $C_{25}H_{52}$ and $C_{33}H_{68}$. As a result, the elastic stiffness constants c_{11} and c_{22} of odd-numbered n-alkanes for $n > 25$ can be predicted approximately.

Table 2. Model calculations concerning the elastic properties along the crystallographic c-axis of $C_{33}H_{68}$ and $C_{25}H_{52}$, using the series connection model described in the text (numbers in square brackets: corresponding references).

	c_{33}^{∞} (GPa)	L_G (nm) (=c)	c_{33} (GPa)	R_I (GPa nm^{-1}) (=c_I/L_I)
$C_{25}H_{52}$	290 [13]	6.70 [5]	35*	11.9**
$C_{25}H_{52}$	305 [14]	6.70 [5]	35*	11.8**
$C_{25}H_{52}$	315 [15]	6.70 [5]	35*	11.7**
$C_{33}H_{68}$	290 [13]	8.765 [3]	43.9***	
$C_{33}H_{68}$	305 [14]	8.765 [3]	44.2***	
$C_{33}H_{68}$	315 [15]	8.765 [3]	44.4***	

* Experimental values.

** Calculated on the basis of equation (4).

*** Calculated on the basis of equation (5), assuming $R_I = 11.8$ GPa nm^{-1}.

For the elastic constant c_{33}, measured for phonon propagation along the molecular chain axis, the experimental values clearly depend on the chain length. Over many decades, a lot of work has been devoted to the determination of the limiting modulus of the single infinite lamella, c_{33}^{∞}. Several groups [12–15] measured LAM modes in n-alkane systems of different chain lengths, and extrapolated the value c_{33}^{∞} for an infinite single lamella on the basis of different models. All groups independently estimated a value of c_{33}^{∞} near 300 GPa (see table 2). The experimental value measured for ultra-drawn polyethylene amounts to 116 GPa [29]. Nevertheless, the experimental values c_{33} for $C_{25}H_{52}$ and $C_{33}H_{68}$ are about one order of magnitude smaller than the limiting value c_{33}^{∞}.

As has already been discussed by Krüger *et al* [16, 17], the weak inter-lamellar interactions are responsible for this renormalization of the limiting modulus of the single infinite lamella, c_{33}^{∞}, down to the measured hydrodynamic low value of c_{33}. As the inter-lamellar interaction forces are of van der Waals type, they strongly reduce the resulting value of c_{33}. It is interesting to compare the experimental value of c_{33} for $C_{33}H_{68}$ with the value estimated by Strobl *et al* about twenty years ago on the basis of their LAM investigations [12, 13]. The experimental value amounts to $c_{33} = 44.2$ GPa, while Strobl *et al* estimated, from the basic LAM mode and its overtones, the elastic constant c_{33} to be 41.7 GPa for $C_{33}H_{68}$. For the estimation of c_{33}, they used the model of a series connection: in the Reuss average [32], a lamellar crystal can be considered from the elastic point of view as a series connection of hard lamellar covalent bonds (elastic modulus c_{33}^{∞}) and soft inter-lamellar van

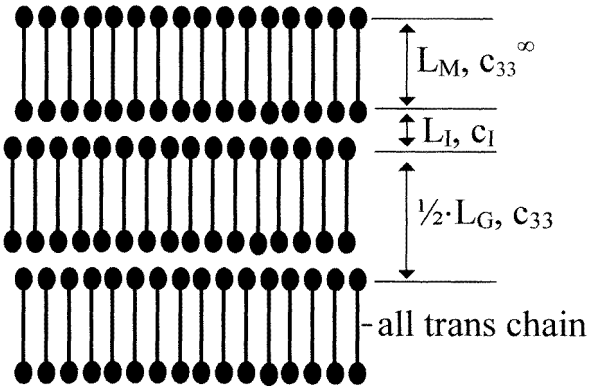

Figure 5. A schematic representation of the series connection model for the determination of the reduced variable $R_I = c_I/L_I$. For further information, see the text.

der Waals bonds (elastic modulus c_I) along the crystallographic c-axis (see figure 5). In such a series connection, the resulting elastic constant is usually governed by the softer bonds, resulting in this low value of $c_{33} = 41.7$ GPa in comparison to c_{33}^{∞} (≈300 GPa). However, their method of estimation of c_{33} was an indirect one, in contrast to our direct Brillouin investigations. Taking this into consideration, our experimental value and the estimated one of Strobl *et al* are in good agreement, and support the idea of approaching the elastic constant c_{33} via a series connection model.

Following such a model of a series connection for phonon propagation along the c-axis—as already proposed by Marx *et al* for the case of perfluoro-alkanes [33]—the elastic modulus for phonon propagation along the c-axis can be tentatively calculated as follows:

$$\frac{L_G}{c_{33}} = \frac{2L_M}{c_{33}^{\infty}} + \frac{2L_I}{c_I} \tag{3}$$

with $L_G = 2L_M + 2L_I$ (=lattice parameter c) according to figure 5, c_I being the modulus of the inter-lamellar layer. As the two quantities c_I and L_I are hardly accessible for n-alkanes, it is convenient to introduce a reduced variable $R_I = c_I/L_I$ [33] as a quantity describing the magnitude of the inter-layer interaction. Making the reasonable assumption that $c_{33}^{\infty} \gg c_I$, equation (3) can be transformed to

$$R_I = \frac{2c_{33}^{\infty}}{L_G}\left(\frac{c_{33}^{\infty}}{c_{33}} - 1\right)^{-1}. \tag{4}$$

On the basis of our experimental data, we estimated R_I in the case of $C_{25}H_{52}$. The values for R_I obtained assuming different values for c_{33}^{∞} [12–15] are given in table 2. As can be seen, the absolute value does not drastically depend on the value of c_{33}^{∞}, and amounts to $R_I \approx 11.8$ GPa nm^{-1}. Since the packing of the inter-lamellar region (AB stacking of adjacent methylene groups) is supposed to be more or less the same for $C_{25}H_{52}$ and $C_{33}H_{68}$, we make the hypothesis that R_I has the same value for the two systems. Then, equation (4) can be transformed for calculating c_{33} in the case of $C_{33}H_{68}$:

$$c_{33} = \frac{c_{33}^{\infty} L_G R_I}{2c_{33}^{\infty} + L_G R_I}. \tag{5}$$

As can be seen from tables 1 and 2, the calculated values are in very good agreement with the experimental ones.

Snyder *et al* [14] found from their investigations that the inter-layer force constant (f_I) should be proportional to $1/n$, where n denotes the number of carbons. In view of this, it is astonishing that we can predict c_{33} with such good accuracy on the basis of our rough model assumptions. Recently, Pietralla *et al* [15] performed a reinvestigation of the LAM modes in n-alkanes including also shorter n-alkanes with n ranging from 20 to 40. As a conclusion, they find that $f_I \propto 1/n$ only holds true for longer n-alkanes ($n > 40$). For the shorter n-alkanes, the force constant tends towards a plateau ($20 < n < 40$).

On the basis of the existing experimental data (two systems) we cannot say whether our rough model assumptions (constant R_I and the series connection model) are in fact correct, or whether we can use equation (5) to predict c_{33} for other n-alkane systems of neighbouring chain lengths also. Nevertheless, we consider equation (5) at least to be a rule of thumb for the estimation of c_{33}. Corresponding investigations to verify the results presented here are planned.

4. Summary

Within this work we have determined and discussed the elastic properties of $C_{33}H_{68}$. Using the PIA technique, we were able to prepare thin crystal mats suitable for investigation with Brillouin spectroscopy. The comparison of the elastic data with those for $C_{25}H_{52}$ revealed interesting results: perpendicular to the molecular chain axes, the elastic data for the two systems correspond to each other. With regard to the findings for ultra-drawn polyethylene, we explain that this is possibly a general feature within the homologue series of n-alkanes ($n > 25$). For sound propagation along the molecular chain axis, the values of the elastic constants c_{33} clearly differ, and are one order of magnitude smaller than the value estimated for an infinite crystal lamella, c_{33}^{∞}. This behaviour can be interpreted on the basis of a dominant role being taken by the weak inter-lamellar van der Waals forces in determining the acoustic properties of n-alkanes. Using a series connection model, we estimate these inter-lamellar van der Waals forces quantitatively in the case of $C_{25}H_{52}$. Making the assumption that the interlayer forces of $C_{25}H_{52}$ and $C_{33}H_{68}$ correspond to each other, we can calculate c_{33} with a very good accuracy. If our rough model assumptions are correct, it should be possible to estimate the elastic constant c_{33} also for other n-alkanes of neighbouring chain lengths. Corresponding investigations will be undertaken.

Acknowledgment

This work was kindly supported by the Deutsche Forschungsgemeinschaft.

References

[1] Broadhurst M G 1962 *J. Res. NBS* A **66** 241
[2] Boistelle R 1980 *Current Topics in Materials Science* vol 4, ed E Kaldis (Amsterdam: North-Holland)
[3] Piesczek W, Strobl G R and Malzahn K 1974 *Acta Crystallogr.* B **30** 1278
[4] Strobl G, Ewen B, Fischer E W and Piesczek W 1974 *J. Chem. Phys.* **61** 5257
[5] Doucet J, Denicolò I, Craievich A F and Collet A 1981 *J. Chem. Phys.* **75** 5125
Denicolò I, Doucet J and Craievich A F 1981 *J. Chem. Phys.* **75** 1523
Denicolò I, Doucet J and Craievich A F 1983 *J. Chem. Phys.* **78** 1465
[6] Ungar G 1983 *J. Phys. Chem.* **87** 689
[7] Doucet J, Denicolò I, Craievich A F and Germain C 1984 *J. Chem. Phys.* **80** 1647
[8] Sirota E B, King H E, Singer D M and Shao H 1993 *J. Chem. Phys.* **98** 5809
[9] Sirota E B and Singer D M 1994 *J. Chem. Phys.* **101** 10 873

[10] Pechhold W, Dollhopf W and Engel A 1966 *Acoustica* **17** 61
[11] Heyer D, Buchenau U and Stamm M 1984 *J. Polym. Sci.* **22** 1515
[12] Strobl G R and Eckel R 1976 *J. Polym. Sci.* **14** 913
[13] Strobl G R 1976 *Colloid Polym. Sci.* **254** 170
[14] Snyder R G, Strauss H L, Alamo R and Mandelkern L 1994 *J. Chem. Phys.* **100** 5422
[15] Pietralla M, Hotz R, Engst T and Siems R 1997 *J. Polym. Sci.* B **35** 47
[16] Krüger J K, Bastian H, Ansbach G I and Pietralla M 1980 *Polym. Bull.* **3** 633
[17] Krüger J K, Pietralla M and Unruh H-G 1982 *Phys. Status Solidi* a **71** 493
[18] Wittmann J C and Smith P 1991 *Nature* **352** 414
[19] Krüger J K, Prechtl M, Smith P, Meyer S and Wittmann J C 1992 *J. Polym. Sci.* B **30** 1173
[20] Krüger J K, Prechtl M, Wittmann J C, Meyer S, Legrand J F and D'Asseza G 1993 *J. Polym. Sci.* B **31** 505
[21] Grammes C, Krüger J K, Bohn K-P, Baller J, Fischer C, Schorr C, Rogez D and Alnot P 1995 *Phys. Rev.* E **51** 420
[22] Krüger J K, Grammes C, Jiménez R, Schreiber J, Bohn K-P, Baller J, Fischer C, Rogez D, Schorr C and Alnot P 1995 *Phys. Rev*. E **51** 2115
[23] Jiménez R, Krüger J K, Prechtl M, Grammes C and Alnot P 1994 *J. Phys.: Condens. Matter* **6** 10 977
[24] Jiménez R, Krüger J K, Fischer C, Bohn K-P, Dvorák V, Holakovský J and Alnot P 1995 *Phys. Rev.* B **51** 3353
[25] Jiménez R, Krüger J K, Bohn K-P and Fischer C 1996 *J. Phys.: Condens. Matter* **8** 7579
[26] Frey H, Sheiko S, Möller M, Wittmann J C and Lotz B 1993 *Adv. Mater*. **5** 917
[27] Fenwick D, Smith P and Wittmann J C 1996 *J. Mater. Sci.* **31** 128
[28] Krüger J K, Heydt B, Fischer C, Baller J, Jiménez R, Servet B, Galtier P, Pavel M , Ploss B, Bottani C and Beghi M 1997 *Phys. Rev.* B **55** 3497
[29] Krüger J K 1989 *Optical Techniques to Characterize Polymer Systems* ed H Bässler (Amsterdam: Elsevier)
[30] Krüger J K, Marx A, Peetz L, Roberts R and Unruh H-G 1986 *Colloid Polym. Sci.* **264** 403
[31] Auld B A 1973 *Acoustic Fields and Waves in Solids* (New York: Wiley)
[32] Reuss A 1929 *Z. Angew. Math. Mech.* **9** 49
[33] Marx A, Krüger J K and Unruh H-G 1989 *Z. Phys.* B **75** 101